Accepted Manuscript

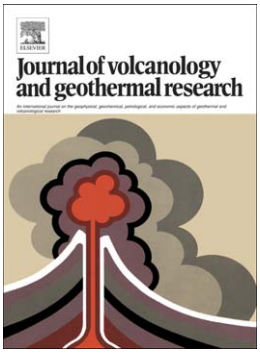

A Statistical Approach to Evaluate the Tephra Deposit and Ash Concentration from Puff Model Forecasts

S. Scollo, M. Prestifilippo, M. Coltelli, R.A. Peterson, G. Spata

PII: S0377-0273(10)00382-3
DOI: doi: 10.1016/j.jvolgeores.2010.12.004
Reference: VOLGEO 4673

To appear in: *Journal of Volcanology and Geothermal Research*

Received date: 2 July 2010
Accepted date: 2 December 2010

Please cite this article as: Scollo, S., Prestifilippo, M., Coltelli, M., Peterson, R.A., Spata, G., A Statistical Approach to Evaluate the Tephra Deposit and Ash Concentration from Puff Model Forecasts, *Journal of Volcanology and Geothermal Research* (2010), doi: 10.1016/j.jvolgeores.2010.12.004

A STATISTICAL APPROACH TO EVALUATE THE TEPHRA DEPOSIT AND ASH CONCENTRATION FROM PUFF MODEL FORECASTS

S. Scollo (1) (*), M. Prestifilippo (1), M. Coltelli (1), R. A. Peterson (2), G. Spata (1)

(1) Istituto Nazionale di Geofisica e Vulcanologia - Sezione Catania, Catania, Italy
(2) Mechanical Engineering, Univ. Alaska, Fairbanks, USA

(*) Corresponding author: Simona Scollo; e-mail: scollo@ct.ingv.it

Manuscript submitted to JVGR

Abstract

In this paper we present a new statistical approach able to provide tephra deposit load and ash concentration using PUFF, a lagrangian model widely used to forecast volcanic ash dispersal during volcanic crisis. We perform a parametric study in order to analyze the influence of each input parameter on model outputs. For this test, we simulate two eruptive scenarios like to the 2001 (*Scenario 1*) and 1998 (*Scenario 2*) Etna eruptions using high resolution weather data and a domain of 170 x 170 km. Results show that for both scenarios, we are able to calculate the tephra deposit load and ash concentration but the use of millions of particles is required. Specifically, up to 33 and 220 millions of particles were necessary to accurately predict the tephra deposit and ash concentration in air, respectively. This is approximately two orders of magnitude larger than values typically considered running PUFF. The parametric study shows that the horizontal diffusion coefficient, the time step of the simulations, the topography and the standard deviation of the particle distribution greatly affect the model outputs. We also validate the model by best fit procedures. Results show a good comparison between field data of the 2001 Etna eruption and PUFF simulations, being inside 5 and 1/5 times the observed data, comparable with results of Eulerian models.
This work will allow to reliably outlining the areas of contaminated airspace using PUFF or any other lagrangian model in order to define the No Fly Zone and ensure the safety to aviation operations as required after the Eyjafjallajökull eruption.

Keywords: ash dispersal; ash forecasting and aviation safety; PUFF model; parametric study and model validation; Mt. Etna.

1. Introduction

Predictive models help significantly in reducing the risk associated with a wide range of different volcanic activities (e.g. Keating et al., 2008). Simultaneously, sensitivity analysis techniques and uncertainty estimation are becoming more prevalent in order to study how the variation in model outputs can be attributed to different sources of variation in model inputs as well as to estimate the model reliability (e.g. Saltelli et al., 2008). For this aim, the use of data obtained by monitoring systems combined with modelling strategies has become an important scientific goal in most of the geophysical communities (Charpentier, 2008).

Volcanic ash released during explosive eruptions can be responsible for severe damage to aircraft, buildings, crops and telecommunications (e.g. Casadewall, 1994). As an example, during the recent Etna eruptions (e.g. 2001 and 2002-03 activities) tephra fallout drastically affected the local economy and transport system (e.g. Barnard, 2004). The mitigation of damage may be assisted by volcanic ash transport and dispersion models (VATDM) that are able to forecast the regions which will be affected by volcanic ash dispersal and fallout. However, it is clear that these models need to be compared with field data in order to estimate the model reliability.

The Istituto Nazionale di Geofisica e Vulcanologia, sezione di Catania (INGV-CT) runs four different tephra dispersal models daily: FALL3D (Costa et al., 2006), HAZMAP (Macedonio et al., 2005), TEPHRA (Bonadonna et al., 2005a), and PUFF (Searcy et al., 1998). The model forecasts are provided every day to the Italian civil protection that prepares for and manages emergencies (Scollo et al., 2009). So far, a parametric study and model validation analysis have only been carried out at Etna for FALL3D (Costa et al., 2006), HAZMAP (Scollo et al., 2007), and TEPHRA (Scollo et al., 2006) by comparing model results with field data from the 2001 Etna eruption. TEPHRA was also validated using data of the 1998 Etna and the 1996 Ruapehu eruptions (Scollo et al., 2008a). The PUFF model has not yet been validated in a similar way.

PUFF is a volcanic ash tracking model initially developed to simulate the movement of volcanic particles through a Lagrangian formulation of advection, fallout and turbulent diffusion based on a random-walk technique. PUFF simulates the paths of N particles and provides forecasts of the location of a given particle size at a specific time instant. In order to compare PUFF simulations with field data, the evaluation of tephra ground accumulation and of ash concentration in air simulated by this code are needed. However, these quantitative outputs are not directly available from PUFF forecasts. An early attempt to make a straight-forward comparison between PUFF forecasts and field data was carried out by Tanaka and Yamamoto (2002) who drew a contour surrounding the ash deposit and counted the mass of particles that fell over a unit area. However, this type of computation has a certain degree of uncertainty. In fact, due to the random processes used in PUFF, one could find a different number of particles in a fixed area and/or volume even if the model runs were performed with the "same" input parameters. Therefore, there is an important issue which should first be addressed: if we run two simulations using the same input parameters

and then we calculate the deposit and/or ash concentration maps, how large are the differences between two simulations?

In this work we follow the Tanaka and Yamamoto (2002) approach and demonstrate that it is possible to reliably estimate the mass over an area or volume unit using the PUFF model. We apply a statistical method to analyze PUFF simulations and evaluate the minimum number of particles (N_m) required for minimizing the differences between two simulations when the same input parameters are used.

In order to apply the proposed method it is necessary to perform a large number of simulations using a reasonable amount of computing time. However, this is easy addressed thanks to the growth in performance and capacity of microprocessors and the advancement in parallel computing tecniques. In fact, parallel computer codes are increasingly being used in Volcanology because they allow simulating the complex physical processes in a brief period of time during an ongoing eruption (for example in 3D pyroclastic flows (e.g. Cavazzoni et al., 2005), and volcanic ash dispersal (e.g. Folch et al., 2008)). In this work a parallelization technique is applied for the first time to PUFF model in order to reduce the time computing.

The goal of this paper is threefold: the first goal is to investigate the ability of PUFF to calculate the deposit load and ash concentration; the second and third goals are to perform a parametric study of input parameters, and the evaluation of the reliability of PUFF outputs through comparisons with field data of a well-studied eruption.

The paper is structured as follows: section 2 describes the method used to calculate the deposit load and ash concentration, to perform the parametric study and model validation; results are presented in section 3, and a discussion and concluding remarks are in sections 4 and 5, respectively.

2. The method

2.1 The eruptive scenarios

In our test, we consider two different eruptive scenarios which are simulated daily at INGV-CT to forecast tephra dispersal from Etna volcano (Scollo et al., 2009). These scenarios represent two different typologies of Etna explosive activity which were observed during the last twenty years. The first scenario is similar to the first phase of 2001 Etna eruption. During this phase the eruption column rose up to 5 km a.s.l. producing a weak and bent over plume continuously for 4 days (Scollo et al., 2007). The second scenario is similar to the explosive event that occurred at Voragine crater on 22 July 1998. The activity produced a strong plume rising about 12 km a.s.l. (Andronico et al., 1999) and represented one of the most powerful episodes observed in the last ten years. The main features of the explosive activity were obtained by the analysis of field data for both the 2001 (hereafter *Scenario 1*) and 1998 (hereafter *Scenario 2*) events, and the input parameters necessary to simulate the dispersal by VATDM (Table 1) were identified for both events (Scollo et al., 2009).

We used *Scenario 1* and *Scenario 2* to perform the following parametric study to PUFF model. *Scenario 1* was also used to apply a model validation technique. In fact, field data of the 2001 Etna eruption (Scollo et al., 2007) has been widely used to validate several volcanic ash transport and dispersion models (FALL3D, HAZMAP, VOL-CALPUFF, TEPHRA) and data are freely available for model validation (http://www.ct.ingv.it/Progetti/Iavcei/index.htm).

2.2 The PUFF model

PUFF simulates the transport, dispersion and sedimentation of volcanic ash by evaluating at any time the position of thousands of particles. The model was initially developed by Tanaka (1994) and Searcy et al. (1998) with the aim of reducing the risk to aviation from volcanic ash encounters in the northwestern Pacific area. It has been operative at the Alaska Volcano Observatory since the eruption of Redoubt volcano in 1989. The original code together with the most recent versions are freely available at the web-site http://puff.images.alaska.edu/downloads.shtml. PUFF forecasts have already been compared with many eruptions from Alaskan and Japanese volcanoes (e.g. Tanaka and Yamamoto, 2002) and used to reproduce the dispersal of volcanic ash from the May 18, 1980 eruption of Mount St. Helens (Fero et al., 2008), the 2001 eruption of Mt. Cleveland (Dean et al., 2004), the eruption of the Crater Peak vent, Mount Spurr, Alaska in August 1992 (Webley et al., 2009), the 1991 eruption of Mt. Pinatubo (Fero et al., 2009), and the 1991 eruption of Mt. Hudson (Kratzmann et al., 2010). For Etna volcano, Aloisi et al. (2002) simulated the dispersal of the paroxysm that occurred on 22 July 1998 and Daniele et al. (2009) evaluated the area around the volcano affected by the presence of volcanic ash during the same event. PUFF is therefore widely used by a large scientific community and has also been operative at INGV-CT since 2006 in order to forecast volcanic ash dispersal during Etna explosive eruptions (Scollo et al., 2009).

In this work, numerical simulations were carried out using PUFF version 2.6. A detailed description of the model can be found in Searcy et al. (1998). Table 2 shows input parameters for PUFF used in our analysis (the italicized terms correspond with the option name within the PUFF code).

Meteorological data are provided by the Italian Air Force Meteorological Office and cover the entire area of Sicily from 12.5° to 18.5° E and from 34.5° to 40.5° N. We use a form of code parallelization known as "data parallelism" in which data are distributed across different parallel computing nodes. In our method, PUFF runs on a cluster composed of 48 nodes and each node produces a number of outputs using a fixed number of volcanic particles. Results of the different simulations are subsequently summed in order to obtain a simulation having a greater number of particles. It is notable that this approach is possible because in the PUFF model there are no interactions between the particles.

2.3 Computation of the tephra deposit and ash concentration

Consider the path of "one" particle computed by PUFF from the eruption column up to the time of deposition on the ground. After a time t the particle will fall onto the location (x_1, y_1) which is a function of

several randomly determined variables (e.g. the initial position of the particle inside the eruption column, the particle size that is a function of the initial grain-size distribution, the random walk due to the turbulence, wind speed and direction). Most variables depend on probabilistic functions, and consequently if we repeat the simulation without any alteration, the new particle location will likely be $(x_2, y_2) \neq (x_1, y_1)$. It is therefore meaningful to pose the question: in a given square (or volume) unit, what is the probability that the particle will fall inside this specified surface (or volume)?

The answer to this question requires the use of a statistical approach. Hereafter we describe the approach for evaluating the mass on a given surface *S* (the deposit load). Similarly the same approach may be applied to evaluate the mass in a given volume *V* (ash concentration).

If *N* represents the number of particles simulated by PUFF, and P_s the probability of finding a particle inside the surface unit *S*, for *N* large enough, the number of particles N_s in *S* is given by *N* x P_s. In our simulations, particles have different sizes. If *c* represents the size classes, N_c the number of particles of size class *c*, and P_c the probability of finding the particle of size class *c* in *S*, the total number N_s of particles in *S* is given by $N_S = \sum_i^c N_i P_i$. We are similarly able to evaluate the total mass falling in *S* by $M_S = \sum_i^c m_i N_i P_i$, where m_i is the mass of particles estimated by the radius of the particles. In PUFF, all particles are, in fact, assumed spherical with the same density (2500 kg/m^3). Keeping the same initial grain-size distribution of the particles, for a large enough value of *N*, there is a linearity between *N* and N_s ($N \propto N_s$), and therefore also proportionality between the total erupted mass *M* and M_s ($M \propto M_s$). Similarly, we can write $M^{ES} \propto M_S^{ES}$ where *ES* is for a particular "eruptive scenario" (in our case M^{ES} is the total mass erupted in *Scenario 1* or *Scenario 2*). Consequently, it is possible to evaluate the mass in *S* (the deposit load) of the real eruptive scenario using $M_S^{ES} = \frac{M^{ES}}{M} \cdot M_S = \gamma \cdot M_S$.

In our study, we run PUFF using a high number of particle size and perform the calculation following these steps: i) define the surface *S* (volume *V*) having a size of 1 km x 1 km (1 km x 1 km x 1 km); ii) calculate the total mass inside the surface (M_s) or volume (M_V); iii) scale this value by the factor γ obtaining the mass on surface *S* (or volume *V*) for a given eruptive scenario M_S^{ES} (M_V^{ES}).

The main problem is: what is the minimum number of particles (N_m) so that this statistical approach is accurate? The basic premise is that we need to increase *N* until the ash concentration in *S* is very near to the value obtained with a different simulation also using the same number *N* of particles.

Next the statistical approach used to find N_m is described. First, we run *r* simulations, each with N_{ini} (the number of particles released by PUFF in each simulation). In our case N_{ini} is equal to 50,000. Consequently, *r* outputs will be generated, each containing N_{ini} particles. These simulations are then taken randomly and summed in order to obtain an output composed of $N_i = i \cdot N_{ini}$ particles with *i* ranging between 1 and any integer positive value. For each N_i, we generate a number of simulations *n* (again taking the previous outputs randomly) and calculate the deposit load (ash concentration). Considering all the possible pairs of

the deposit load (ash concentration) generated using n simulations, we evaluate the correlation coefficient $\rho^{i}_{p,q}$ (relative to the pair (p, q) and number of particles N_i) that is a measure of the relative stability of the result:

$$\rho^{i}_{p,q} = \frac{\mathrm{cov}(R_p, R_q)}{\sigma_p \sigma_q} = \frac{E\{(R_p - \mu_p)(R_q - \mu_q)\}}{\sigma_p \sigma_q} \quad (1)$$

where R is the vectorized map concentration (the column vector obtained using the vectorization of the matrix of ash concentration) and μ and σ are respectively the mean value and the standard deviation of the vector R. If the simulations are similar, the value of $\rho^{i}_{p,q}$ approaches to 1. Furthermore, the mean value and standard deviation of $\rho^{i}_{p,q}$ is evaluated for each N_i. For simplicity, we may make a new vectorization of the matrix having elements $\rho^{i}_{p,q}$ obtaining a vector with elements ρ^{i}_{j} (with j=1.. $n_i(n_i - 1)/2$).

As an example, suppose that we run r = 8 simulations with N_{ini} = 50,000 labeled as: *a*, *b*, *c*, *d*, *e*, *f*, *g*, *h*. If the maximum value of i is fixed to 5, N_i could vary between 50,000 and 250,000 (50,000 x 5). Consider N_3 = 150,000 (that is generated by summing 3 runs randomly), we may choose to generate n = 4 simulations by summing 3 runs randomly, for example: A = [a b f]; B = [c d a], C = [d e h]; D = [a e g]. Now, the correlation coefficient ρ^{3}_{j} may be evaluated taking all the combinations (AB, AC, AD, BC, BD, CD) obtaining 4 x (4-1)/2 = 6 correlation values. Finally, we evaluate the mean value and the standard deviation using these six values of ρ^{3}_{j}. This approach is then repeated for each value of N_i. In our analysis, we ran r = 200 simulations fixing N_{ini} = 50,000 in each separate run. These simulations are taken randomly and summed in order to obtain values of N_i ranging between 50,000 and 7,500,000 with step of 50,000. For each value of N_i, we generate n = 20 simulations so that we have 190 values of ρ^{i}_{j} (20 x (20-1)/2). Furthermore, we calculate the mean value (μ^i) and the standard deviation (σ^i) of ρ^{i}_{j} (with respect to j). Using 190 values of ρ^{i}_{j}, the mean value of ρ^{i}_{j} for each N_i is approximated using the function: $\rho^{i}_{j} = N_i/(N_i + a)$. The minimum number of particles (N_m) is then estimated to reach the stability of the final result. In our study, this is obtained when ρ^{i}_{j} = 90%, 95% and 99%. Further, using N_m, the deposit load (ash concentration) is evaluated.

It should be noted that the choice of a cell with side of 1 km was mainly related to reach high resolution simulations. However, our results may be extended to a coarser mesh using the "Parzen Windows" approach (Duda et al., 2001). Following this approach, the surface S (volume V) changes with the number of particles as $1/\sqrt{N_m}$. Hence, if we use a cell with side of 5 km maintaining the same domain (170 km x 170 km), the N_m necessary to reach the same stability will be N_m /625 (N_m /15625 for the volume).

2.4 Parametric study and model validation

We performed a parametric study of input parameters in order to evaluate the difference between two simulations of the tephra deposit due to the variation of each input parameter for *Scenario 1* (*S1*) and *Scenario 2* (*S2*). We changed input parameters of *S1* (Table 3) and *S2* (Table 4) and for each sample of inputs, we calculate N_m and the deposit load (ash concentration). Given two simulations with vectorized map concentration R_i and R_j, their difference is quantified using:

$$J_{i,j} = \frac{\frac{1}{W}\sum (R_i - R_j)^2}{\sqrt{\frac{1}{W}\sum R_i^2 \cdot \frac{1}{W}\sum R_j^2}} \qquad (2)$$

where W is the number of grid points in the mesh or the length of the vectors R_i and R_j.

When $J_{i,j}$ is near 0 the runs are similar, and consequently the variation due to a specific input parameter does not significantly affect the result. Following the approach of Scollo et al. (2009), we classify the difference between two runs as low if $\Delta \leq 0.33$, moderate if $0.33 < \Delta \leq 0.66$, high if $0.66 < \Delta \leq 0.99$ and extreme if $\Delta \geq 1$.

Model validation was carried out in order to find input parameters of the PUFF model that fit better the 2001 field data. The complete description of the eruption and analysis of the field data can be found in Scollo et al. (2007). Input parameters were changed following the same table used for the previous parametric study of *S1* (Table 3) and the simulation results were compared with field data by a standard best fit function (e.g. Bonadonna et al., 2002).

3 Results

3.1 Tephra deposit load and Ash concentration computation

For each scenario, we evaluate the values of N_m required to reach 90%, 95% and 99% of ρ_j^i on the ground and at 1828 m (FL60, where FL indicates the flight level), at 3657 m (FL120) and at 5486 m (FL180) above sea level. Figure 1 shows the number of particles N_m required to reach 99% of ρ_j^i for *S1* and using input parameters as described in Table 3. It is notable that if the value of *dtMins* is equal to 5 or 10 (S1-RUN9-1, S1-RUN9-2), a great number of particles are necessary to reach convergence. Setting this parameter to 1 improves the Lagrangian method, so we recommend that large values of *dtMins* should be avoided. Furthermore, high value of N_m occurred increasing the values of the standard deviation of the total grain-size distribution (S1-RUN2-3, S1-RUN2-4) and excluding the topography (S1-RUN11-1).

In particular, we found that for S1-RUN0, 99% of ρ_j^i is reached on the ground using only 5.2 M (million) of particles (Figure 2). However, a greater number of particles are needed for FL60, FL120 and FL180 levels being about 130 M, 56 M and 250 M respectively (Figure 1). It is notable also that a large number of particles are required at FL180 probably because only a small number of the total particles reach this upper elevation.

Scenario 2 has similar features to *Scenario 1*. Figure 3 shows the number of particles N_m necessary to reach 99% of ρ_j^i for *S2* using input parameters as described in Table 4. Again, the standard deviation of the total grain-size distribution (S2-RUN2-3, S2-RUN2-4), the time step (S2-RUN9-1, S2-RUN9-2) and the topography (S1-RUN11-1) affect the value of N_m. There is also an increase in N_m with an increase in the mean of the total grain-size distribution (S2-RUN1-1 and S2-RUN1-2).

Figure 4 shows the ρ_j^i plot as a function of N_i for S2-RUN0 and the computation of ρ_j^i at 95% on the ground. It is obtained using about 4.7 M particles, whereas 24 M particles are necessary to increase ρ_j^i to 99% (Figure 3).

Table 5 shows N_m (averaged over all runs from RUN0 to RUN11), for *S1* and *S2* on the ground and at FL60, FL120 and FL180. It is notable that N_m increases with the increase of the correlation coefficient (ρ_j^i=99%). The convergence of 90% and 95% is reached with a number of particles less than about 7 M on the ground and less than about 45 M at different flight level for both scenarios. Furthermore, except for the deposit load, *S1* needs a greater number of particles to calculate the ash concentration at different flight levels than *S2* (about 5 times more). We note that the convergence is obtained easily in those regions where a large number of particles are present and it is strictly linked to input parameters used in the simulations.

Figure 5 shows the comparison between the computed deposits using 50,000 particles and 5.2 M particles for S1-RUN0 and Figure 6 using 50,000 and 4.6 M particles for S2-RUN0. Increasing the number of particles clearly causes a decrease in the noise and a stabilization of deposit load (ash concentration) maps.

Finally, it is highlighted that N_m may change with respect to the weather conditions. Simulations were carried out for S1-RUN0 using the forecasting weather data of 10 November 2007 between 3:00 and 6:00 AM and 6 August 2007 between 3:00 and 6:00 AM, days that were characterized by high speed winds (75 and 98 knts at 3000 and 5000 m) and near-zero wind, respectively. In these dramatically different weather conditions, we found a difference in N_m of about 30%.

3.2 The parametric study

Table 6 shows the results of the parametric study for *S1*. It is carried out changing the input parameters (Table 3 and 4) and comparing the computed deposit between two simulations by (2). All these runs were carried out with the maximum number of particles (7.5 M particles). It is remarkable that extreme differences occur if we introduce the topography (DEM) and change the *diffuseH* and *dtMins* parameters.

Regarding the use of a DEM, it is notable that the top of Etna with its steep slopes and 3350 m a.s.l. elevation strongly affects the local wind circulation (Favalli et al, 2004). Results in Table 6 show that PUFF is very sensitive to this parameter and similar results would be expected for most other volcanoes having a complex orography like Etna. The *diffuseH* parameter defines the horizontal diffusion coefficient (m^2/s) used in the random-walk method of diffusion. When the horizontal diffusion is near 0, the lateral spreading of volcanic clouds occurs only by wind advection. This parameter has an important role on the volcanic ash dispersal and should be set accurately.

The parameter *dtMins* controls the time step of the simulations. The default value is 10 minutes, but smaller value should be used in order to obtain finer time results. Quantitatively, the previous analysis has shown that the value should be set to 1 (chapter 3.1). If not, the computational time required due to the necessary large value of N_m, could be unmanageable. Table 6 shows that the standard deviation of the particle distribution also has an important effect on the final results. The variation of the standard deviation modifies the size distribution of volcanic particles and consequently the terminal settling velocity distribution. The particle velocity can follow different laws: 1) the Stokes law with a constant air viscosity ("*Constant*" option); ii) the Stokes law in which the effect of pressure and temperature on air viscosity is accounted for ("*Stokes"* option); iii) an empirical function of the particle Reynold's number ("*Reynolds"* option) as suggested in Bonadonna et al. (1998). As expected, these variations cause extreme differences in the forecasted deposit because terminal settling velocity has an important effect on sedimentation processes (e.g. Pfeiffer et al., 2005). This conclusion is also confirmed by increasing the percentage of fine particles in the total grain-size distribution, which results in large differences as seen in Table 6.

Table 7 shows the results for *S2*. Both the *diffuseH* and *dtMins* parameters have an important effect on the computed dispersal and deposit. The use of the DEM has instead a secondary effect. This is expected for eruption columns which have heights of several kilometers due to the fact that volcanic particles have to travel a longer distance from the initial volcanic plume to the ground in *S2*. For the same reason, the model of the terminal settling velocity has a major influence and consequently should be as accurate as possible. It is notable that while errors up to 2 ϕ (ϕ is for $-\log_2 d$, where d is the diameter in mm) for *ashLogMean* parameter are low or moderate (Table 7) the *ashLogSdev* parameter has a major effect on the deposit. Furthermore, the *plumeShape* parameter describing the initial distribution of particles inside the column may play an important effect on the deposition for this scenario.

For both scenarios, the effect of the variation in the vertical diffusion coefficient is relatively irrelevant. The parameter was varied between 0.001 and 100 but substantial differences with RUN0 were not observed. We also found that the model is not sensitive to *plumeHwidth,* indicating that the ash plume is advected in a very similar manner within the same grid cell. Instead, *plumeZwidth* (the initial vertical depth of the cloud) may more substantially affect the pattern deposition for both scenarios. This is in agreement with Webley et al. (2009) who found that the accuracy of the vertical distribution is important in the initial source condition.

3.3 Model Validation

We perform a best-fit procedure in order to find the input parameters of PUFF which give a better agreement with the field data of the 2001 Etna eruption (Scollo et al., 2007). Input parameters were modified following Table 3, and for each run we calculate the deposit and perform the best fit procedure. Results are shown in Table 8. We found the optimal *ashLogMean* parameter is equal to -3.9 (0.125 mm/3 ϕ) and *ashLogSdev* equal to 0.3 (0.5 mm/1 ϕ), implying finer grain-size than Scollo et al. (2007). An initial column height of 5500 m gives the best fit in agreement with observations carried out by MISR (Scollo et al., 2010). The best fit for the initial particle distribution is a linear distribution. Similarly, for the same eruption, the results of the HAZMAP model show the maximum concentration of the total mass located at the middle of the eruption column and not concentrated around the maximum (Scollo et al., 2007).

It is notable that the best description of the sedimentation is obtained using the "Reynolds settling law". At the moment it is the best settling description available in PUFF as it accounts for the most of the complex dynamics of volcanic ash fallout. Further, the time step is set to 1 min and the use of an accurate DEM gives the best results (as we expected for an eruption producing a weak plume). Figure 7 shows the comparison between the PUFF simulation using the best fit values and the field data of the 2001 explosive event. Results show that all points are inside 5 and 1/5 times the observed data. These results are hence comparable with those obtained by other tephra dispersal models like HAZMAP and FALL3D (see Scollo et al., 2008b).

4. Discussion

4.1 The Number of Particles

In this analysis, we tested the ability of PUFF to compute the deposit load and ash concentration. Using two standard scenarios for the eruptive behavior of Etna, we found that the ash concentration can be computed using millions of particles. Consequently, we are now able to compare the PUFF results with field data of any eruption and\or results of other VATDM (e.g. FALL3D). PUFF is a Lagrangian model and has been used to date for particle tracking to provide ash dispersal forecasts for explosive eruptions. However, we have demonstrated that by applying an appropriate statistical approach, the model may be used in much the same way as any other numerical model (e.g. Eulerian models).

In order to apply the proposed statistical approach, it is necessary to greatly increase the number of particles N from the default value to N_m. However, N may change with the differing characteristics of different eruptions, computational domains, and meteorological conditions. Consequently, N_m should be evaluated any time the initial conditions are significantly modified. In our case, we identified two different scenarios, *Scenario 1* and *Scenario 2*, run daily at INGV-CT for forecasting Etna volcanic plumes (Scollo et al., 2009). Consequently we fixed both sets of input parameters and the computational domain.

It should be noted that *Scenario 2* represents one of the most explosive events that has occurred in the last century at Etna volcano. We found that, for a similar event, about 33 M particles should be used to reach the

99% of the correlation coefficient on the ground (Table 5). This is probably due to the fact that most of particles could be out the domain or still in air after three hours of simulation. This could explain why a smaller number of particles in air are needed in *S2* with respect to *S1*. Since this event was sub-plinian in style (Andronico et al., 1999), for volcanic eruptions having a higher intensity (e.g. August 1991, Hudson volcano, Chile, (Kratzmann et al, 2010)), N_m should be increased even only accounting for the necessary increase of the computational area. In our case the computed area is 170 x 170 km^2. VATDM usually use a larger domain (order of 1500 x 1500 km^2). Consequently, if the explosive activity is increasing and we are interested in investigating a wider domain, we expect the number of particles to increase greatly keeping the same grid resolution. However, it is difficult to make a correlation between N_m and increasing of explosive activity because in our study *S1* and *S2* differ for intensity of explosive activity but also for the duration (3 h for *S1* and 5 min for *S2*).

In PUFF, N is set at 5,000 particles by default. However, many users in previous analyses increase the number of particles up to 100,000 particles (Fero et al., 2008, 2009). Webley et al. (2007) showed that PUFF is an efficient tool for simulating the distribution of atmospheric ash cloud for small eruptions over short time periods using 10,000 particles, averaged over 10 simulations. In agreement with Peterson and Dean (2003), the choice of N is a tradeoff between physical representation and computational requirements. In order to calculate the deposit load and ash concentration, N has to be at least two orders of magnitude higher than the previous applications. This requires the use of parallel computing techniques that are capable of making this work manageable. This analysis was made possible using a Beowulf cluster composed of 48 nodes at INGV-CT. In this way, a PUFF output containing 7.5 M volcanic particles is obtained in only a few minutes.

Peterson and Dean (2003) found that the number of simulations necessary to create a suitable average among PUFF simulations produced from the random-walk process was 50. In our analysis, we average 190 values of ρ_j^i taking the combination of all possible pairs of 20 simulations (section 2.2). This leads to the question of what happens if 190 different simulations are taken instead of combinations. Therefore, we performed the following test.

We ran 190 simulations for S1-RUN0 (FL120) each having 20 M particles (obtained by summing 400 "different" runs with 50,000 particles). In this case, the correlation was 94.97%. Instead, using 20 M particles obtained by combinations, the correlation was 97%. Consequently, with respect to our forecast, we have an error of only about 2%. If the volcanic particles are further increased to 40 M, the correlation is 97.84% whereas the estimated value is 98.5%. As expected, our results improve by increasing the number of particles.

Finally, we remark that, from the operational point of view, after the Eyjafjallajökull eruption, there is the necessity to evaluate the areas of low ($\leq 2 \times 10^{-3}$ g/m^3), medium ($\geq 2 \times 10^{-3}$ g/m^3 and $\leq 4 \times 10^{-3}$ g/m^3) and high ash contaminations ($\geq 4 \times 10^{-3}$ g/m^3) as required in the Volcanic Ash Contingency Plan of Europe and North Atlantic Regions (ICAO, 2010). Presently, the PUFF outputs are useless to define the unsafe areas if it is applied as a particle tracking model. The proposed approach allows to obtain quantitative ash

concentration maps from PUFF outputs (and any Lagrangian model), useful to define the No Fly Zone and mitigating the risk caused by volcanic ash encountering.

4.2 The parametric study

The *diffuseH* parameter (the horizontal diffusion) has a first order effect on the PUFF results for both scenarios. The default horizontal diffusion coefficient is a conservative 10,000 m^2/s because PUFF was designed as an operational ash dispersal forecasting tool. Searcy et al. (1998) found a value of 8000 m^2/s in order to match the eruption of Rabaul Caldera on 14 September 1994, and a value of 5000 m^2/s was required to model the Etna eruption on 22 July 1998 (Daniele et al., 2009). Analyzing the dispersal of volcanic ash from Usu volcano in Japan on 31 March 2000, Tanaka and Yamamoto (2002) found a value of 100 m^2/s. Due to these different results, it is very difficult to determine predefined values of *diffuseH*. Consequently, it should be evaluated during the eruption in order to furnish the best fit with the observations because our parametric study demonstrates how this input has a strong influence on the forecasted deposition. We suggest that a preliminary matching between PUFF simulations and satellite images could furnish a preliminary value for *diffuseH*.

The *dtMins* parameter used in the Lagrangian time-stepping method should be set near 1 min. This parameter is strictly linked to the eruptive scenarios considered in the study. The only advantage in increasing the value of *dtMins* is the consequent decrease in computational time required (Peterson and Dean, 2003). However, parallel computing techniques, as used in this analysis, drastically reduce this time.

Topography influences the time at which the particle reaches the ground. For weak plumes, the topography parameter (DEM) plays an important role due to the slower travelling of volcanic particles from plume to the ground. The effect should decrease with the increase of the initial column height. Our results confirm a stronger influence of the DEM for weak plumes produced by *S1* than strong plumes produced by *S2* (Table 6 and Table 7).

The *ashLogMean* parameter describes the grain-size distribution of volcanic particles. Peterson and Dean (2003) showed that particle size has the most dramatic effect on model results. However, our tests show that the *ashlogSdev* parameter (standard deviation of the Gaussian particle size distribution) has a greater effect than the *ashLogMean* parameter for both two scenarios. This effect increases with the decreasing of the particle size in agreement with Peterson and Dean (2003) who found small changes in the standard deviation have relatively large effects when the particle size is small.

The *plumeMax* parameter has a small influence on the PUFF results. However, we considered an error in the estimation of the column height of only ± 1 km because the good monitoring of Etna plumes (e.g. Andronico et al., 2009) allow constraining this parameter with a fairly high degree of precision through images mainly obtained from video surveillance carried out by INGV-CT. Results are in agreement with Scollo et al. (2009) findings that small variations of the column height have little influence on the model outputs of HAZMAP, TEPHRA and FALL3D models. It should be highlighted that the uncertainty in plume heights for other volcanoes which are less well monitored than Etna could have more important implications on plume dispersal (Papp et al., 2005).

PUFF has three different options for describing the settling terminal velocities of volcanic ash ("*Constant"*, "*Stokes"*, and "*Reynolds"*). In particular, results show that the choice of the three different model options may modify the PUFF results for eruptions having high initial eruption columns. Several studies have

shown that terminal settling velocity law has an important role in the pattern of deposition (e.g. Pfeiffer et al., 2005) and should be modeled accurately. Hence, in our opinion, due to the importance of the Reynolds number on the thickness variations of tephra fall deposits (Bonadonna et al., 1998), the "*Reynolds*" law is the preferred description. It is also notable that PUFF does not account for two important phenomena that are very common in sedimentation processes of volcanic ash: i) the decreasing in terminal settling velocities due to the irregular shape of volcanic ash (e.g. Riley et al., 2003; Coltelli et al., 2008); ii) the presence of an aggregation phenomenon (e.g. Durant et al., 2009). The first should decrease terminal velocity values whereas the latter could lead to the premature fallout of fine ash.

The *plumeShape* parameter (describing the particle distribution within the eruption column) influences the results only for *S2*. In agreement with Peterson and Dean (2003), it should be chosen accurately if eruptions produce a strong plume. However, in the case of Etna, the majority of events in the last ten years produced weak plumes (Andronico and Scollo, 2008) and this parameter may be considered less consequential. Differences in the model results could be due to the variation of the particle distribution inside the column. In the literature, there are several empirical methods used in ash dispersal modeling to distribute the mass along the eruption column (e.g. Suzuki, 1983). However, these empirical laws should be revised and replaced with more reliable models on eruption column distributions already available in the literature (e.g. Ishimine, 2007).

4.3 The Best-fit

The field data of 2001 Etna eruption (Scollo et al., 2007) have extensively been used to evaluate the performance of VATDM as FALL3D (Costa et al., 2006), VOL-CALPUFF (Barsotti and Neri, 2008), and HAZMAP (Scollo et al., 2007). Further, input parameters of this event have recently been considered as a representative scenario for Etna volcano (Mastin et al., 2009) by the Eruption Source Parameters workgroup (http://esp.images.alaska.edu/index.php). These data are therefore ideal to test the reliability of PUFF model forecasts. Results show that the best fit is obtained using a fine grain-size class reflecting the phreatomagmatic nature of the first phase of Etna eruption (Scollo et al., 2007). The best fit for the maximum column height is 5.5 km. As previously mentioned, this result is very similar to those obtained by analyzing the MISR images (Scollo et al., 2010), whereas it is higher with respect to the maximum column height obtained by the geometric analysis of pictures taken during the explosive event (Scollo et al., 2007). However, it is noted that while the error of the MISR height ranges from 0.1 to a maximum of 0.4 km (Naud et al., 2004), the error in the column height observed in the field may reach 1 km. PUFF also describes well the distribution of particles inside the eruption column. We found in fact that the linear distribution leads to a good fit to the real tephra deposit. In agreement with models of well mixed weak plumes, such as the 2001 event, the rising plume is subjected to a turbulently diffused vertical current in which particles are distributed almost uniformly in the vertical direction due to a more efficient turbulent mixing and vorticity (Turner, 1973; Bonadonna et al., 2005b).

Lagrangian models such as PUFF are widely used by volcanic ash advisory centers (VAAC) to reduce risks from volcanic ash dispersal. However, they are usually run with a relatively small number of particles

forcing them to obtain only qualitative information from model results. Instead, our results show that when the number of particles is increased, we can calculate the tephra deposit and ash concentration in air reliability. Results of best-fit procedure demonstrate that a Lagrangian model can furnish the same information as an Eulerian model, making possible any comparisons among model results.

5. Concluding remarks

This work shows that, using a statistical approach, we can calculate tephra deposit load and ash concentration in air by a Lagrangian model such as PUFF. We find that for two well defined eruption scenarios and a small computation domain, up to 33 and 220 million particles are necessary to accurately calculate the deposit load and ash concentration in air, respectively. These values are at least two orders of magnitude larger than the values typically considered by Lagrangian models. Despite the high number of particles, the computational time may be drastically reduced using parallel computing techniques. Consequently, lagrangian models could be used to define the volumes of airspace which should be interdicted to aviation operations and improve current strategies of ash forecasting.

The parametric analysis has shown that PUFF results are greatly affected by the topography, the horizontal diffusion coefficient, the time step of the simulations, and the standard deviation of the particle distribution. While the topography needs to be included and the time step can be set to the minimum value, the horizontal coefficient and the standard deviation should be set accurately when PUFF is used operationally during emergencies.

Finally, a comparison between PUFF simulations and the 2001 field data has shown that PUFF may furnish reliable values of the deposit load comparable with results obtained by other volcanic ash dispersal models.

In future, additional tests should be carried out in order to better evaluate how the minimum number of particles N_m is affected by the eruption size. Finally, a detailed comparison between a Lagrangian (e.g. PUFF) and Eulerian model (e.g. FALL3D) should be performed in a way to evaluate the strength and weakness of the two different approaches.

The proposed approach will allow to obtain quantitative ash concentration maps from Lagrangian model such us PUFF which are widely used by VAACs to forecast volcanic ash dispersal and define the contaminated area for ensuring the safety of the air transportation.

Acknowledgements

The authors thank M. Aloisi for his advices in running PUFF model and A. Bonaccorso who encouraged the use of PUFF as operative tool for Etna volcanic ash forecasting. The authors thank to the reviewers Arnau Folch and Costanza Bonadonna that improved the quality of the paper with their constructive suggestions. The native speaker Stephen Conway is also thanked. This work was funded by the FIRB Italian project ‘‘Sviluppo Nuove Tecnologie per la Protezione e Difesa del Territorio dai Rischi Naturali’’ of Italian Minister of University and Research for three of the authors (M. Prestifilippo, S. Scollo, G. Spata).

Figures

Figure 1. Log of the minimum number of particles (N_i) required to reach the 99% of ρ_j^i on the ground and at different flight levels (FL60, FL120, FL180) for *Scenario 1*.

Figure 2. Correlation coefficient (ρ_j^i) in function of the number of particles (N_i) for *Scenario 1*. The yellow circle shows the number of particles necessary to reach the 99% of ρ_j^i on the ground. The mean value (μ^i) and the standard deviation (σ^i) of ρ_j^i are plotted using the black and broken blue line, respectively. The red line represents the mean value of ρ_j^i evaluated by $\rho_j^i = N_i/(N_i + a)$.

Figure 3. Log of the minimum number of particles (N_i) required to reach the 99% of ρ_j^i on the ground and at different flight levels (FL60, FL120, FL180) for *Scenario 2*.

Figure 4. Correlation coefficient (ρ_j^i) in function of the number of particles (N_i) for *Scenario 2*. Color lines as described in Figure 2.

Figure 5. Comparison between the computed deposits using 50,000 particles (top) and 5.2 M of particles for S1-RUN0 (bottom).

Figure 6. Comparison between the computed deposits using 50,000 particles (top) and 4.7 M of particles for S2-RUN0 ((bottom).

Figure 7. Comparison between the simulation using the values obtained by the best-fit procedure and the field data at each sampling point (kg m^{-2}) of the 2001 Etna eruption (Scollo et al., 2007). The equiline represents an ideal line if a perfect agreement exists, the dotted lines marks the region between 5 and 1/5 times the observed mass at each station.

Tables

References

Aloisi, M., D'Agostino, M., Dean, K.G., Mostaccio, A., Neri, G., 2002. Satellite analysis and PUFF simulation of the eruptive cloud generated by the Mount Etna paroxysm of 22 July 1998. J. Geophys. Res. 107 (B12), doi: 10.1029/2001JB000630.

Andronico, D., Del Carlo, P., Coltelli, M., 1999. The 22 July 1998 fire fountain episode at Voragine Crater (Mt. Etna, Italy). Proceedings of the Volcanic and Magmatic Studies Group - Annual Meeting. January 5–6, 1999.

Andronico, D., Scollo, S., 2008. 1998–2007: Ten years of explosive activity at Mt. Etna volcano, IAVCEI 2008 General Assembly, Reykjavìk, Island, 18-24 August 2008.

Andronico, D., Scollo, S., Cristaldi, A., and Ferruccio, F., 2009. Monitoring ash emission episodes at Mt. Etna: The 16 November 2006 case study. J. Volcanol. Geoth. Res. 180, 123-134.

Barnard, S. T., 2004. Results of a reconnaissance trip to Mt. Etna, Italy: The effects of the 2002 eruption of Etna on the province of Catania. Bull. New Zealand Soc. Earthquake Eng. 37 (2), 47-62.

Barsotti, S., Neri, A., 2008. The VOL-CALPUFF model for atmospheric ash dispersal: 2. Application to the weak Mount Etna plume of July 2001. J. Geophys. Res. 113, B03209, doi: 10.1029/2006JB004624.

Bonadonna, C., Ernst, G. G. J., Sparks, R. S. J., 1998. Thickness variations and volume estimates of tephra fall deposits: the importance of particle Reynolds number. J. Volcanol. Geotherm. Res. 81, 173–187.

Bonadonna, C., Macedonio, G., Sparks, R. S. J., 2002. Numerical modelling of tephra fallout associated with dome collapses and Vulcanian explosions: application to hazard assessment on Montserrat. In: lDruitt, T.H., Kokelaar, B.P. (Eds.), The Eruption of Soufrière Hills Volcano, Montserrat, from 1995 to 1999. Geological Society, London, pp. 517–537. Memoir.

Bonadonna, C., Connor, C. B., Houghton, B. F., Sahetapy-Engel, S., Hincks, T., Connor, L., 2005a. Probabilistic modeling of tephra dispersion: hazard assessment of a multi-phase rhyolitic eruption at Tarawera,NewZealand. J. Geophys. Res. 110, B03203. doi:10.1029/2003JB002896.

Bonadonna, C., Phillips, J. C., Houghton, B. F., 2005b. Modeling tephra sedimentation from a Ruapehu weak plume eruption. J. Geophys. Res. 110, B08209. doi:10.1029/2004JB003515.

Casadevall, T. J., 1994. Volcanic ash and aviation safety. Proceedings of the First International Symposium on Volcanic Ash and Aviation Safety. U.S. Geological Survey Bulletin 2047, 450.

Cavazzoni, C., Ongaro, T. E., Erbacci, G., Neri, A., Macedonio, G. 2005. High performance computing simulations of pyroclastic flows, Computer Physics Communications 169, 454-456.

Charpentier, I., 2008. Variational coupling of Plinian column models and data: Application to El Chichon volcano, J. Volcanol. Geotherm. Res. 175, 501-508.

Coltelli, M., Miraglia, L., Scollo, S., 2008. Shape characterization of the volcanic particles carried out by SEM technique for the calculus of the terminal settling velocities. Bull. Volcanol. doi: 10.1007/s00445-007-0192-8.

Costa, A., Macedonio, G., Folch, A., 2006. A three dimensional Eulerian model for transport and deposition of volcanic ashes. Earth Planet. Sci. Lett. 241, 634–647.

Daniele, P., Lirer, L., Petrosino, R., Spinelli, N., Peterson, R., 2009. Applications of the PUFF model to forecasts of volcanic clouds dispersal from Etna and Vesuvio. Comput. Geosci. 35, 1035-1049.

Dean, K. G., Dehn, J., Papp, K. P., Smith, S., Izbekov, P., Peterson, R., Kearney, C., Steffke, A., 2004. Integrated satellite observations of the 2001 eruption of Mt. Cleveland, Alaska. J. Volcanol. Geotherm. Res. 135, 51–73.

Duda, R. O., Hart P. E., Stork D.G., 2001. Pattern classification. Wiley, 2 edition, November 2001.

Durant, A. J., Rose, W. I., Sarna-Wojcicki, A. M., Carey, S., Volentik, A. C. M., 2009. Hydrometeor-Enhanced Tephra Sedimentation: Constraints from the 18 May 1980 Eruption of Mount St. Helens (USA). J. Geophys. Res. 114, doi: 10.1029/2008JB005756.

Favalli, M., Mazzarini, F., Pareschi M. T., Boschi, E, 2004. Role of local wind circulation in plume monitoring at Mt. Etna volcano (Sicily): Insights from a mesoscale numerical model. Geophys. Res. Lett. 31, doi: 10.1029/2003GL019281.

Fero, J., Carey, S. N., Merrill, J. T., 2008. Simulation of the 1980 eruption of Mount St. Helens using the ash-tracking model PUFF. J. Volcanol. Geotherm. Res. 175 (3), 355–366.

Fero, J., Carey, S. N., Merrill, J. T., 2009. Simulating the dispersal of tephra from the 1991 Pinatubo eruption: implications for the formation of widespread ash layers. J. Volcanol. Geotherm. Res. 186 (1–2), 120–131.

Folch, A., Cavazzoni, C., Costa, A., Macedonio G., 2008. An automatic procedure to forecast tephra fallout. J. Volcanol. Geotherm. Res. 177, 767– 777.

Keating, G. N., Pelletier, J. D., Valentine, G. A., Statham, W., 2008. Evaluating suitability of a tephra dispersal model as part of a risk assessment framework, J. Volcanol. Geotherm. Res. 177, 397– 404.

Kratzmann, D. J., Carey, S., Scasso, R., Naranjo, J. A., 2010. Simulations of tephra dispersal from the 1991 explosive eruptions of Hudson volcano, Chile. J. Volcanol. Geotherm. Res. 190, 337– 352.

ICAO, 2010. EUR Doc 019 NAT Doc 006, Part II. Volcanic Ash Contingency Plan, Eur and Nat Regions. July 2010.

Ishimine, Y., 2007. A simple integral model of buoyancy-generating plumes and its application to volcanic eruption columns. J. Geophys. Res. 112, B03210, doi: 10.1029/2006JB004274.

Macedonio, G., Costa, A., Longo, V., 2005. A computer model for volcanic ash fallout and assessment of subsequent hazard. Comput. Geosci. 31, 837–845.

Mastin, L. G., Guffanti, M., Servranckx, R., Webley, P., Barsotti, S., Dean, K., Durant, A., Ewert, J. W., Neri, A., Rose, W. I., Schneider, D., Siebert, L., Stunder, B., Swanson, G., Tupper, A., Volentik, A., Waythomas, C. F. 2009. A multidisciplinary effort to assign realistic source parameters to models of volcanic ash-cloud transport and dispersion during eruptions. J. Volcanol. Geotherm. Res. 186, 10-21.

Naud, C., Muller, J., Haeffelin, M., Morille, Y., Delaval, A., 2004. Assessment of MISR and MODIS cloud top heights through intercomparison with a back-scattering lidar at SIRTA. Geophys. Res. Lett. 31, L04114, doi:10.1029/2003GL018976.

Papp, K. R., Dean, K. G., Dehn, J., 2005. Predicting regions susceptible to high concentrations of airborne volcanic ash in the North Pacific region. J. Volcanol. Geotherm. Res. 148, 295–314.

Peterson, R. A., Dean K., 2003. Sensitivity of Puff: a Volcanic Ash Particle Tracking Model, Technical Report (http://puff.images.alaska.edu/sensitivity/sens_paper.pdf).

Pfeiffer, T., Costa, A., Macedonio, G., 2005. A model for the numerical simulation of tephra fall deposits. J. Volcanol. Geotherm. Res. 140 (4), 273–294.

Riley, C. M., Rose, W. I., Bluth, G. J. S., 2003. Quantitative shape measurements of distal volcanic ash. J. Geophys. Res. 108 (B10), 2504, doi:10.1029/2001JB000818.

Saltelli, A., Ratto, M., Andres, T., Campolongo, F., Cariboni, J., Gatelli, D., Saisana, M., Tarantola, S., 2008. Global Sensitivity Analysis the Primer, John Wiley & Sons.

Scollo, S., Bonadonna, C., Coltelli ,M., Del Carlo, P., 2006. Probabilistic tephra fall-hazard assessment at Etna volcano, Italy, Cities on Volcanoes 4, Quito, Ecuador, 22–27 January 2006.

Scollo, S., Del Carlo, P., Coltelli, M., 2007. Tephra fallout of 2001 Etna flank eruption: analysis of the deposit and plume dispersion. J. Volcanol. Geoth. Res. 160, 147–164.

Scollo, S., Tarantola, S., Bonadonna, C., Coltelli, M., Saltelli, A., 2008a. Sensitivity analysis and uncertainty estimation for tephra dispersal models. J. Geophys. Res. 113 (B06202), doi: 10.1029/2006JB004864.

Scollo, S., Folch, A., Costa, A., 2008b. A parametric and comparative study of different tephra fallout models. J. Volcanol. Geotherm. Res. 176, 199–211.

Scollo, S., Prestifilippo, M., Spata, G., D'Agostino, M., Coltelli, M., 2009. Monitoring and forecasting Etna volcanic plumes. Nat. Hazards Earth Syst., 9, 1573-1585.

Scollo, S., Folch, A., Coltelli, M., Realmuto, V.J., 2010. 3D volcanic aerosol dispersal: a comparison between misr data and numerical simulations. J. Geophys. Res., in print.

Searcy, C., Dean, K., Stringer, W., 1998. PUFF: a high-resolution volcanic ash tracking model, J. Volcanol. Geotherm. Res. 80, 1–16.

Suzuki, T., 1983. A theoretical model for dispersion of tephra. In: D.S.a.I.Y. (Ed.), Arc Volcanism, Physics and Tectonics. Terra Scientific Publishing Company Terra Scientific Publishing Company Terrapub, Tokyo, pp. 95–113.

Tanaka, H. L., 1994. Development of a prediction scheme for volcanic ash fall from Redoubt volcano, Alaska, Proc. First International Symposium on Volcanic Ash and Aviation Safety, U.S. Geological Survey, Bulletin 2047, 283–291.

Tanaka, H. L., Yamamoto, K., 2002. Numerical simulation of volcanic plume dispersal from Usu Volcano in Japan on 31 March 2000 using PUFF model. Earth Planets Space 54 (7), 743–752.

Turner, J. S., 1973. Buoyancy Effects in Fluids. Cambridge University, Press, Cambridge, pp. 368.

Webley, P. W., Dean, K., Bailey, J. E., Dehn, J., Peterson, R., 2007. Volcanic ash modeling for North Pacific volcanoes automated operational monitoring and virtual globes. 4th International Workshop on Volcanic Ash. Civil Aviation Authority, Rotorua, New Zealand, pp. 1–7.

Webley, P. W., Stunder, B. J. B., Dean, K. G., 2009. Preliminary sensitivity study of eruption source parameters for operational volcanic ash cloud transport and dispersion models — a case study of the August 1992 eruption of the Crater Peak vent, Mount Spurr, Alaska. J. Volcanol. Geotherm. Res. 186 (1–2), 108–119.

Table 1

	Scenario 1 (S1)	***Scenario 2 (S2)***
Eruption Duration	3 h	5 min
Erupted Mass (kg)	$\sim 10^9$	$\sim 1.3\times 10^9$
Averaged Mass Flow Rate (kg/s)	5×10^4	1×10^6
Plume Height (km)	4.5	11
Duration of simulation	3 h	3 h

Table 2

Input Parameters	
N	Number of particles released by PUFF in each simulation
ashLogMean	Base-10 log of the mean particle size (m)
ashLogSdev	Standard deviation of the Gaussian distribution (m)
plumeMax	Maximum plume height (m)
plumeHwidth	Initial horizontal width of the cloud (km)
plumeShape	Vertical distribution of particles within the initial eruption column. It can be a linear, poissonian or exponential distribution
plumeZwidth	Initial vertical depth of the cloud (km) within which the ash particles are initially distributed
diffuseZ	Vertical diffusion coefficient (m^2/s)
diffuseH	Horizontal diffusion coefficient (m^2/s)
dtMins	Time step in the lagrangian time-stepping method (min)
sedimentation	Settling law which may be a constant laminar sedimentation (*constant*), pressure and temperature dependent air viscosity with laminar sedimentation (*stokes)* and a variable flow regime dependent on the particle's Reynolds's number (*reynolds*)
topography	Digital elevation model (DEM)

Table 3

S1-RUN	*ashLog Mean*	*ashLog Sdev*	*plume Max*	*plumeH width*	*plume Shape*	*plumeZ width*	*diffuse Z*	*diffuse H*	*dt Mins*	*sedimen tation*	*topogra phy*
S1-RUN0	-3.6 (2 ϕ)	0.45	4500	0.001	Linear	1	10	10000	1	Reynolds	DEM
S1-RUN1-1	-3 (0 ϕ)	0.45	4500	0.001	Linear	1	10	10000	1	Reynolds	DEM
S1-RUN1-2	-3.3 (1 ϕ)	0.45	4500	0.001	Linear	1	10	10000	1	Reynolds	DEM
S1-RUN1-3	-3.9 (3 ϕ)	0.45	4500	0.001	Linear	1	10	10000	1	Reynolds	DEM
S1-RUN1-4	-4.2 (4 ϕ)	0.45	4500	0.001	Linear	1	10	10000	1	Reynolds	DEM
S1-RUN2-1	-3.6	0.3	4500	0.001	Linear	1	10	10000	1	Reynolds	DEM
S1-RUN2-2	-3.6	0.6	4500	0.001	Linear	1	10	10000	1	Reynolds	DEM
S1-RUN2-3	-3.6	1	4500	0.001	Linear	1	10	10000	1	Reynolds	DEM
S1-RUN2-4	-3.6	2	4500	0.001	Linear	1	10	10000	1	Reynolds	DEM
S1-RUN3-1	-3.6	0.45	3500	0.001	Linear	1	10	10000	1	Reynolds	DEM
S1-RUN3-2	-3.6	0.45	5500	0.001	Linear	1	10	10000	1	Reynolds	DEM
S1-RUN4-1	-3.6	0.45	500	0.01	Linear	1	10	10000	1	Reynolds	DEM
S1-RUN4-2	-3.6	0.45	500	0.1	Linear	1	10	10000	1	Reynolds	DEM
S1-RUN4-3	-3.6	0.45	500	1	Linear	1	10	10000	1	Reynolds	DEM
S1-RUN4-4	-3.6	0.45	500	10	Linear	1	10	10000	1	Reynolds	DEM
S1-RUN5-1	-3.6	0.45	500	0.001	Exponential	1	10	10000	1	Reynolds	DEM
S1-RUN5-2	-3.6	0.45	500	0.001	Poisson	1	10	10000	1	Reynolds	DEM
S1-RUN6-1	-3.6	0.45	500	0.001	Poisson	0.001	10	10000	1	Reynolds	DEM
S1-RUN6-2	-3.6	0.45	500	0.001	Poisson	0.0	10	10000	1	Reynolds	DEM
S1-RUN6-3	-3.6	0.45	500	0.001	Poisson	0.1	10	10000	1	Reynolds	DEM
S1-RUN7-1	-3.6	0.45	500	0.01	Linear	1	0.001	10000	1	Reynolds	DEM
S1-RUN7-2	-3.6	0.45	500	0.01	Linear	1	0.01	10000	1	Reynolds	DEM
S1-RUN7-3	-3.6	0.45	500	0.01	Linear	1	0.1	10000	1	Reynolds	DEM
S1-RUN7-4	-3.6	0.45	500	0.01	Linear	1	1	10000	1	Reynolds	DEM
S1-RUN7-5	-3.6	0.45	500	0.01	Linear	1	100	10000	1	Reynolds	DEM
S1-RUN8-1	-3.6	0.45	500	0.01	Linear	1	10	10	1	Reynolds	DEM
S1-RUN8-2	-3.6	0.45	500	0.01	Linear	1	10	100	1	Reynolds	DEM
S1-RUN8-3	-3.6	0.45	500	0.01	Linear	1	10	1000	1	Reynolds	DEM
S1-RUN8-4	-3.6	0.45	500	0.01	Linear	1	10	Turbulent	1	Reynolds	DEM
S1-RUN9-1	-3.6	0.45	500	0.01	Linear	1	10	10000	5	Reynolds	DEM
S1-RUN9-2	-3.6	0.45	500	0.01	Linear	1	10	10000	10	Reynolds	DEM
S1-RUN10-1	-3.6	0.45	500	0.01	Linear	1	10	10000	1	Constant	DEM
S1-RUN10-2	-3.6	0.45	500	0.01	Linear	1	10	10000	1	Stokes	DEM
S1-RUN11-1	-3.6	0.45	500	0.01	Linear	1	10	10000	1	Reynolds	No DEM

Table 4

S2-RUN	*ashLog Mean*	*ashLog Sdev*	*plume Max*	*plume H width*	*plume Shape*	*plume Z width*	*diffuse Z*	*diffuse H*	*dt Mins*	*sedimentation*	*topography*
S2-RUN0	-3.15 (0 ϕ)	0.45	11000	0.001	Linear	1	10	10000	1	Reynolds	DEM
S2-RUN1-1	-2.7 (-1 ϕ)	0.45	11000	0.001	Linear	1	10	10000	1	Reynolds	DEM
S2-RUN1-2	-2.3 (-2 ϕ)	0.45	11000	0.001	Linear	1	10	10000	1	Reynolds	DEM
S2-RUN1-3	-3.3 (1 ϕ)	0.45	11000	0.001	Linear	1	10	10000	1	Reynolds	DEM
S2-RUN1-4	-3.6 (2 ϕ)	0.45	11000	0.001	Linear	1	10	10000	1	Reynolds	DEM
S2-RUN1-5	-3.9 (3 ϕ)	0.45	11000	0.001	Linear	1	10	10000	1	Reynolds	DEM
S2-RUN1-6	-4.2 (4 ϕ)	0.45	11000	0.001	Linear	1	10	10000	1	Reynolds	DEM
S2-RUN2-1	-3.15	0.3	11000	0.001	Linear	1	10	10000	1	Reynolds	DEM
S2-RUN2-2	-3.15	0.6	11000	0.001	Linear	1	10	10000	1	Reynolds	DEM
S2-RUN2-3	-3.15	1	11000	0.001	Linear	1	10	10000	1	Reynolds	DEM
S2-RUN2-4	-3.15	2	11000	0.001	Linear	1	10	10000	1	Reynolds	DEM
S2-RUN3-1	-3.15	0.45	10000	0.001	Linear	1	10	10000	1	Reynolds	DEM
S2-RUN3-2	-3.15	0.45	12000	0.001	Linear	1	10	10000	1	Reynolds	DEM
S2-RUN4-1	-3.15	0.45	11000	0.01	Linear	1	10	10000	1	Reynolds	DEM
S2-RUN4-2	-3.15	0.45	11000	0.1	Linear	1	10	10000	1	Reynolds	DEM
S2-RUN4-3	-3.15	0.45	11000	1	Linear	1	10	10000	1	Reynolds	DEM
S2-RUN4-4	-3.15	0.45	11000	10	Linear	1	10	10000	1	Reynolds	DEM
S2-RUN5-1	-3.15	0.45	11000	0.001	Exponential	1	10	10000	1	Reynolds	DEM
S2-RUN5-2	-3.15	0.45	11000	0.001	Poisson	1	10	10000	1	Reynolds	DEM
S2-RUN6-1	-3.15	0.45	11000	0.001	Poisson	0.001	10	10000	1	Reynolds	DEM
S2-RUN6-2	-3.15	0.45	11000	0.001	Poisson	0.01	10	10000	1	Reynolds	DEM
S2-RUN6-3	-3.15	0.45	11000	0.001	Poisson	0.1	10	10000	1	Reynolds	DEM
S2-RUN7-1	-3.15	0.45	11000	0.01	Linear	1	0.001	10000	1	Reynolds	DEM
S2-RUN7-2	-3.15	0.45	11000	0.01	Linear	1	0.01	10000	1	Reynolds	DEM
S2-RUN7-3	-3.15	0.45	11000	0.01	Linear	1	0.1	10000	1	Reynolds	DEM
S2-RUN7-4	-3.15	0.45	11000	0.01	Linear	1	1	10000	1	Reynolds	DEM
S2-RUN7-5	-3.15	0.45	11000	0.01	Linear	1	100	10000	1	Reynolds	DEM
S2-RUN8-1	-3.15	0.45	11000	0.01	Linear	1	10	10	1	Reynolds	DEM
S2-RUN8-2	-3.15	0.45	11000	0.01	Linear	1	10	100	1	Reynolds	DEM
S2-RUN8-3	-3.15	0.45	11000	0.01	Linear	1	10	1000	1	Reynolds	DEM
S2-RUN8-4	-3.15	0.45	11000	0.01	Linear	1	10	Turbulent	1	Reynolds	DEM
S2-RUN9-1	-3.15	0.45	11000	0.01	Linear	1	10	10000	5	Reynolds	DEM
S2-RUN9-2	-3.15	0.45	11000	0.01	Linear	1	10	10000	10	Reynolds	DEM
S2-RUN10-1	-3.15	0.45	11000	0.01	Linear	1	10	10000	1	Constant	DEM
S2-RUN10-2	-3.15	0.45	11000	0.01	Linear	1	10	10000	1	Stokes	DEM
S2-RUN11-1	-3.15	0.45	11000	0.01	Linear	1	10	10000	1	Reynolds	No DEM

Table 5

	G	*FL60*	*FL120*	*FL180*
S1-90%	0.6	13.9	6.9	19.9
S1-95%	1.3	29.5	14.6	41.9
S1-99%	7.3	153.5	76.1	219.8
S2-90%	2.9	2.3	1.7	2.6
S2-95%	6.2	5.1	3.7	5.5
S2-99%	32.5	26.1	19.2	28.9

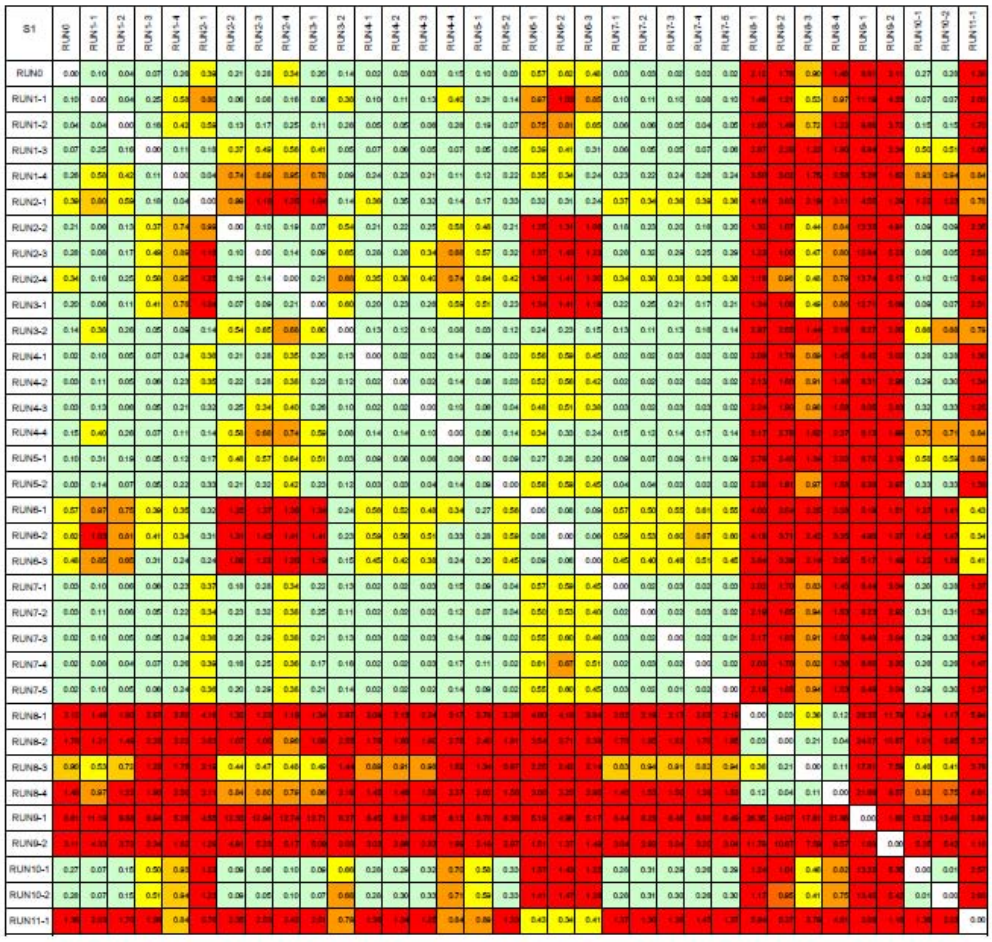

Table 6

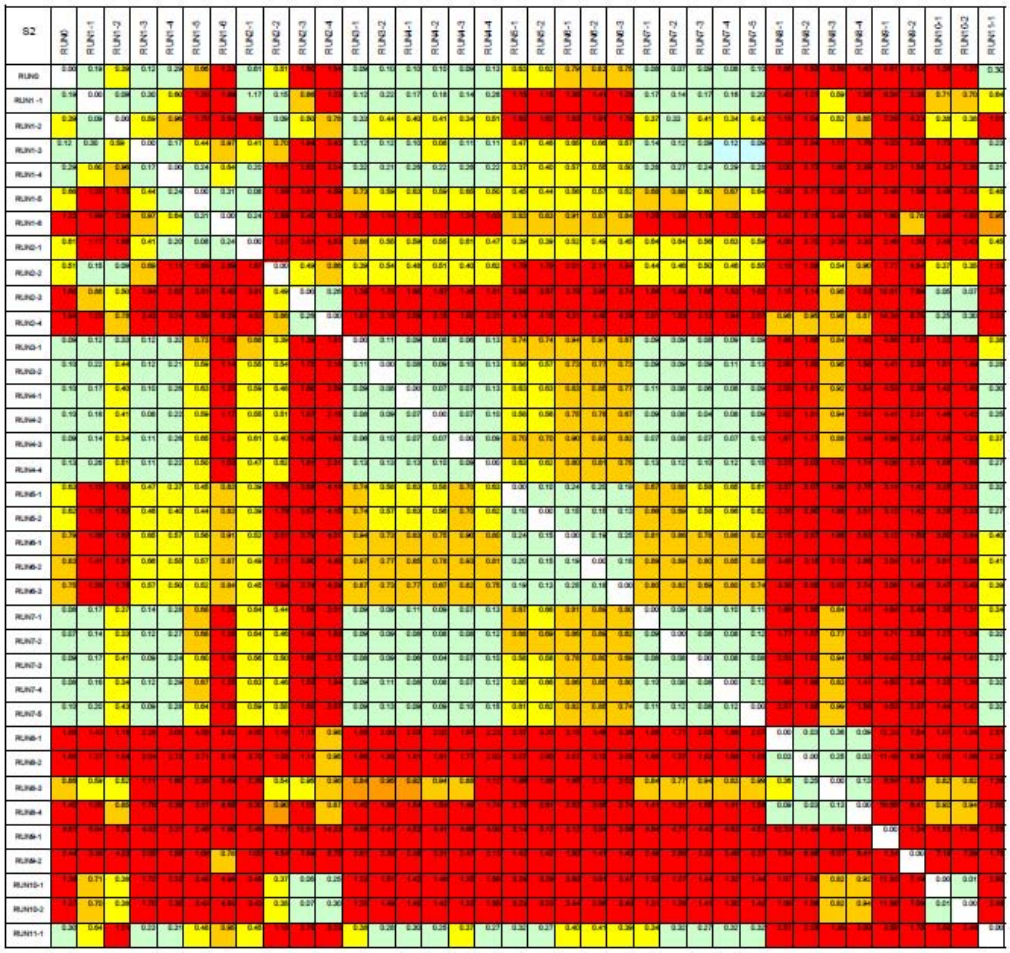

Table 7

Table 8

ashLogMean	-3.9
ashLogSdev	0.3
plumeMax	5500
plumeShape	linear
plumeZwidth	0.1
plumeHwidth	0.01
diffuseZ	1
diffuseH	1000
sedimentation	Reynolds
dtMins	1
DEM	gtopo30

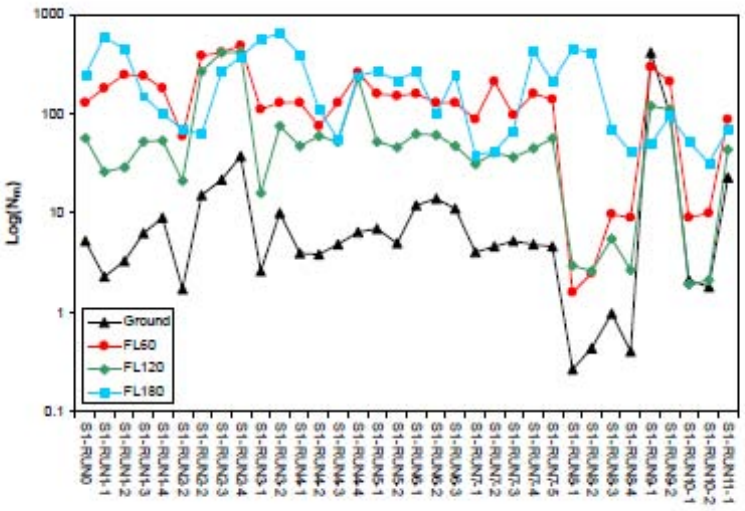

Fig. 1

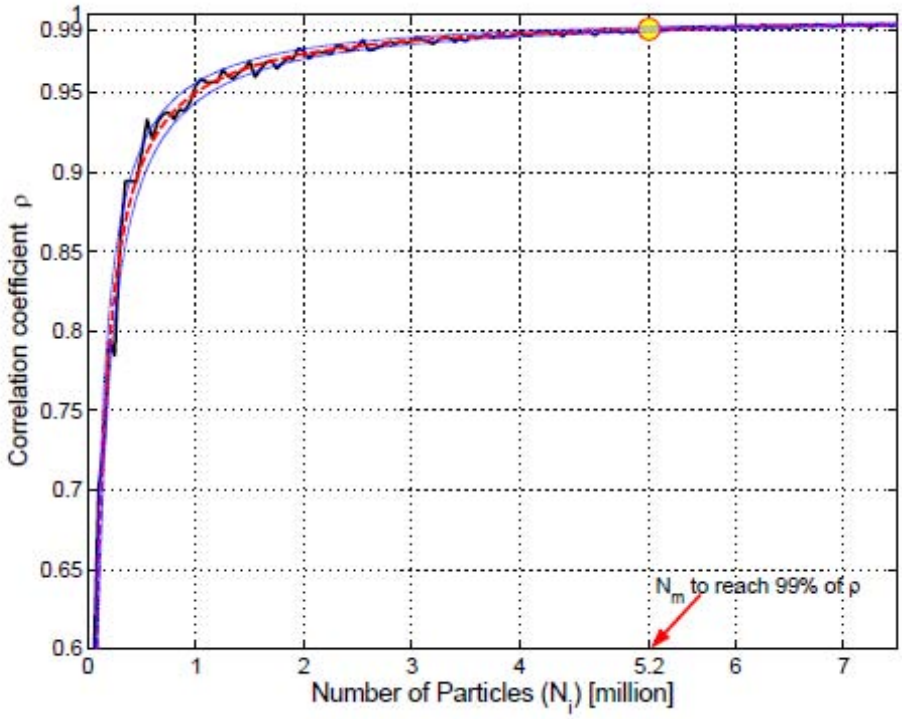

Fig. 2

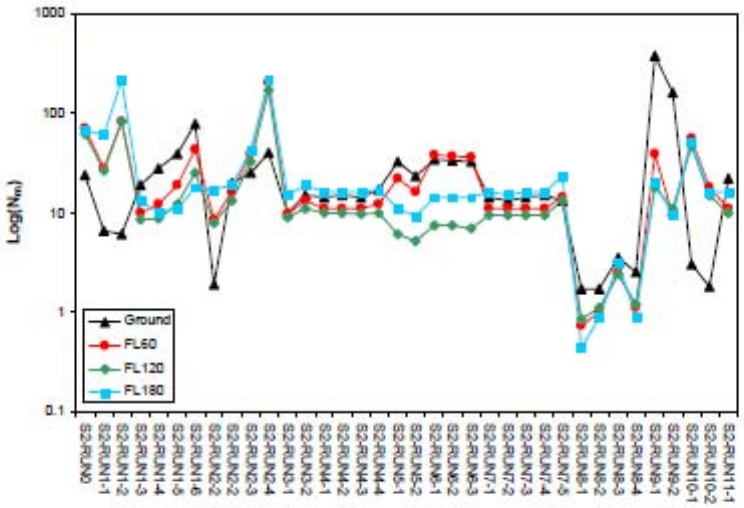

Fig. 3

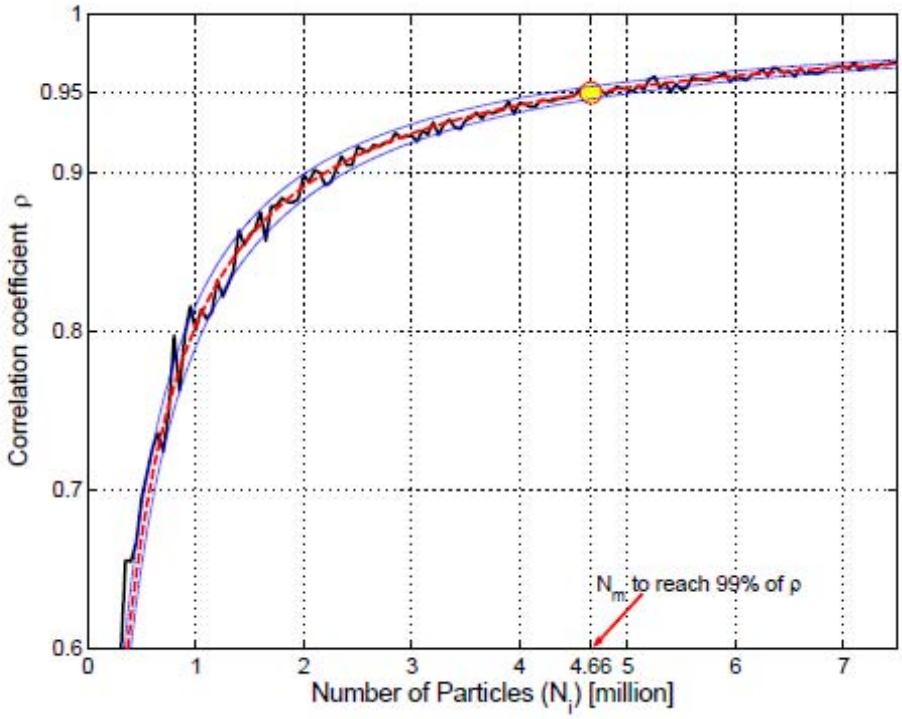

Fig. 4

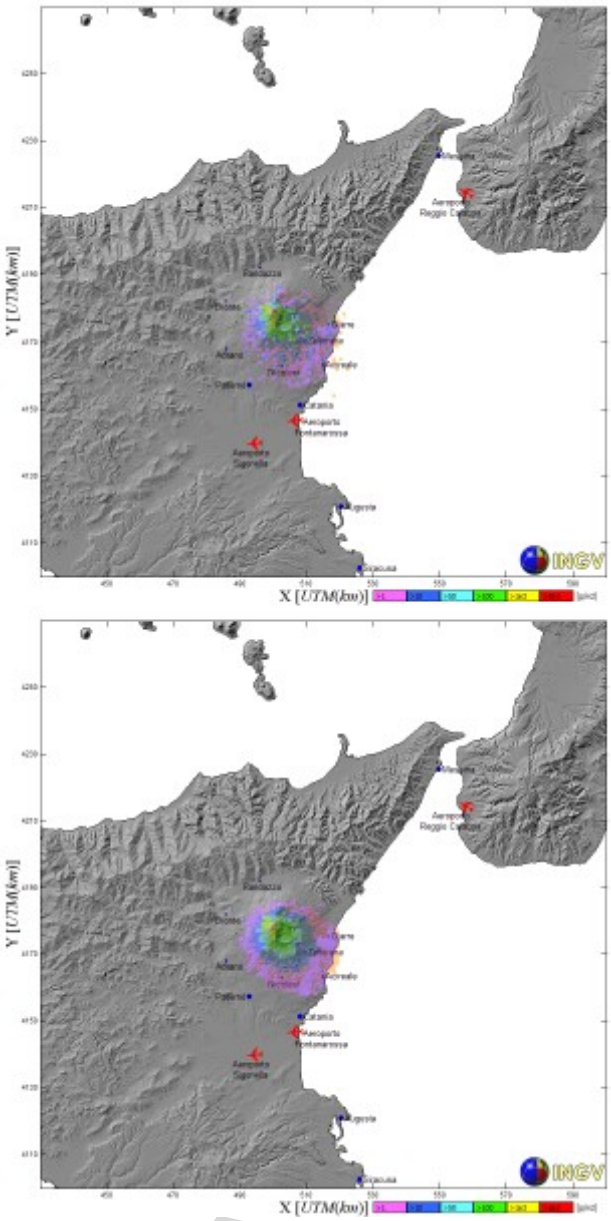

Fig. 5

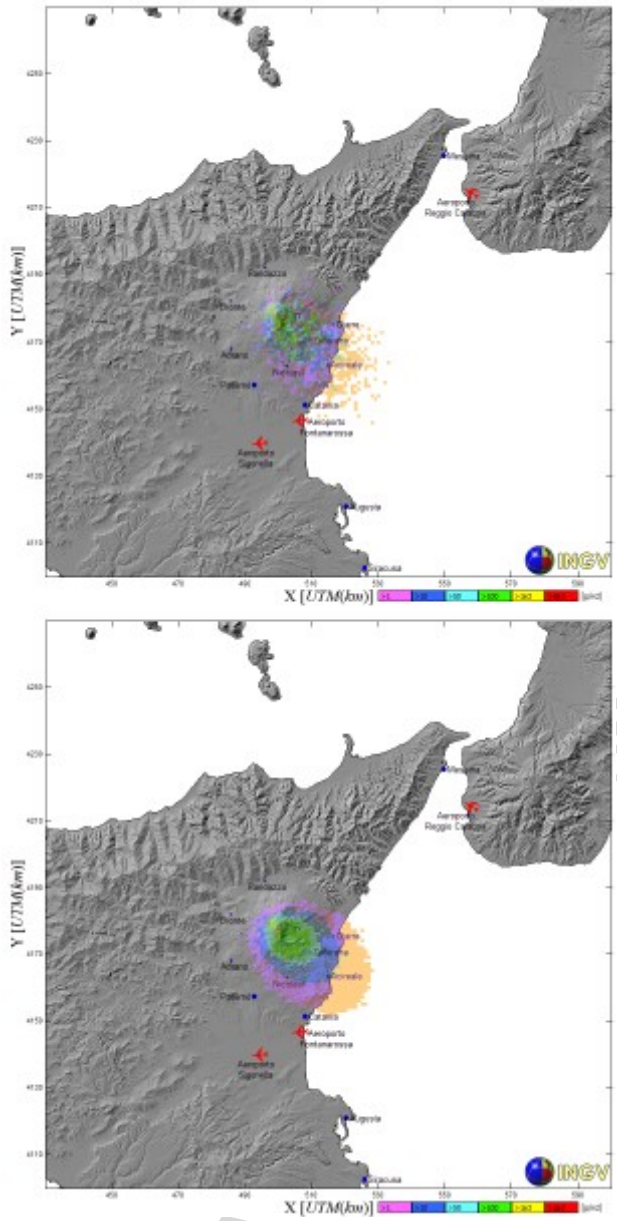

Fig. 6

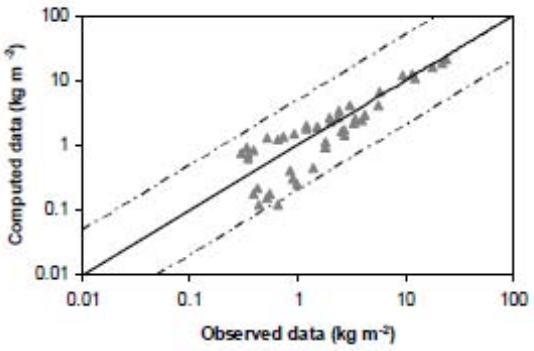

Fig. 7

Research Highlights

1) Tephra deposit and ash concentration may be computed by lagrangian models such us PUFF using a statistical approach;
2) Millions of particles are necessary to accurately predict the tephra deposit and ash concentration in air;
3) Horizontal diffusion coefficient, the time step of the simulations, the topography and the standard deviation of the particle distribution greatly affect the PUFF outputs;
4) Comparison between PUFF simulations and field data of the 2001 Etna eruption shows that PUFF furnishes reliable values of the deposit load comparable with results obtained by other volcanic ash dispersal models;
5) The proposed approach allows to reliably outlining the areas of contaminated airspace using PUFF or any other lagrangian model in order to define the No Fly Zone and ensure the safety to aviation operations.